

Electrical, Electronics and communications, and Computer Engineering

Anti-Disturbance Compensator Design for Unmanned Aerial Vehicle

Ibraheem Kasim Ibraheem
University of Baghdad, College of
Engineering, Department of
Electrical Engineering, Al-Jadriyah,
P.O.B.: 47273, 10001 Baghdad, Iraq;
ibraheemki@coeng.uobaghdad.edu.iq

ABSTRACT

In this paper, an Anti-Disturbance Compensator is suggested for the stabilization of a 6-DoF quadrotor Unmanned Aerial vehicle (UAV) system, namely, the Improved Active Disturbance Rejection Control (IADRC). The proposed Control Scheme rejects the disturbances subjected to this system and eliminates the effect of the uncertainties that the quadrotor system exhibits. The complete nonlinear mathematical model of the 6-DoF quadrotor UAV system has been used to design the four ADRCs units for the attitude and altitude stabilization. Stability analysis has been demonstrated for the Linear Extended State Observer (LESO) of each IADRC unit and the overall closed-loop system using Hurwitz stability criterion. A minimization to a proposed multi-objective Output Performance Index (OPI) is achieved in the MATLAB environment to tune the IADRCs parameters using Genetic Algorithm (GA). The IADRC has been tested for the 6-DOF quadrotor under different tracking scenarios, including disturbance rejection and uncertainties elimination and compared with nonlinear and linear PID controllers. The simulations showed the excellent performance of the proposed compensator against the controllers used in the comparison.

Keywords: Quadrotor; Active disturbance rejection; UAV; Extended State observer; Hurwitz Stability; unmanned aerial vehicle; trajectory tracking; wind disturbance

تصميم معوض مضاد للاضطرابات للمركبة الجوية غير المأهولة

إبراهيم قاسم إبراهيم
أستاذ مساعد
جامعة بغداد
كلية الهندسة
قسم الهندسة الكهربائية

*Corresponding author

Peer review under the responsibility of University of Baghdad.

<https://doi.org/10.31026/j.eng.2020.01.08>

2520-3339 © 2019 University of Baghdad. Production and hosting by Journal of Engineering.

This is an open access article under the CC BY4 license <http://creativecommons.org/licenses/by/4.0/>.

Article received: 14/6/2019

Article accepted: 18/5/2019

Article published: 1/1/2020



الخلاصة

في هذه الورقة، يُقترح معوض مضاد للاضطرابات من أجل تثبيت نظام للمركبات الجوية بدون طيار رباعي الاتجاه (UAV) رباعي الدوران، أي التحكم المحسن في رفض الإزعاج. يرفض مخطط التحكم المقترح الاضطرابات التي يتعرض لها هذا النظام ويزيل تأثير الشوك التي يظهرها النظام رباعي. استخدمنا النموذج الرياضي غير الخطي الكامل لنظام الطائرات بدون طيار رباعي المحركات لتصميم وحدات ADRC الأربعة لتحقيق الاستقرار في منظومات الموقف والارتفاع. لقد تم إثبات تحليل الثبات للمراقب الخطي الممتد (LESO) لكل وحدة من وحدات IADRC ونظام الحلقة المغلقة الشامل باستخدام معيار الاستقرار Hurwitz. يتم تحقيق الحد الأدنى لمؤشر أداء المخرجات متعدد الأهداف (OPI) المقترح في بيئة MATLAB لضبط معلمات IADRC باستخدام الخوارزمية الجينية (GA). تم اختبار IADR التحكم المحسن في رفض الإزعاج في ظل سيناريوهات تتبع مختلفة بما في ذلك رفض الاضطرابات وإزالة الشوك ومقارنتها مع وحدات التحكم PID غير الخطية والخطية. أظهرت المحاكاة الأداء الممتاز للمعوض المقترح ضد وحدات التحكم المستخدمة في المقارنة. **الكلمات الرئيسية:** رفض اضطراب نشط، الطائرات بدون طيار، مراقب الدولة الموسعة، مركبة جوية بدون طيار، تتبع المسار، اضطراب الرياح.

1. INTRODUCTION

The quadrotor is an Unmanned Aerial Vehicle (UAV) that has four motors. Every two motors that are facing each other rotate in the counter-clockwise direction, whereas the other two motors rotate in the opposite direction of the first two motors (clockwise direction). The UAV quadcopter system has six degrees of freedom, three rotations about the Cartesian coordinates, called the attitude. Moreover, an altitude in the vertical direction and movement in two directions called the x-y positioning. Consequently, the motors are less than the number of degrees of freedom. For that reason, it is considered as a severely underactuated system. In recent years, quadrotor applications are increased because of its simplicity, low cost, different sizes for different applications, and easy to be implemented. There are a large variety of civil and military applications for quadrotors. Some of these applications are in research and education purposes (Belyavskiy, et al., 2017), healthcare (Dhivya and Premkumar, 2017), traffic monitoring (Abdullah, et al., 2015), and multi-agent applications (Nathan, et al., 2011). These applications and many others need high maneuverability of the quadrotor and robustness of the control concerning disturbances such as wind and uncertainties such as actuator faults.

Many studies have been done to overcome the disturbances and uncertainties that the quadrotor face during the mission while keeping its motion stable. Controllers such as linear PID has been proposed, but the performance was limited (Sahul, et al., 2014). The best way to deal with these problems is to estimate the disturbances, and many researchers have done this by proposing an observer-based control design (Jingjit, et al., 2014; Aboudonia, Rashad, et al., 2015; Wang and Chen, 2016). Another widely used approach is the active disturbance rejection control (ADRC), it makes use of an Extended State Observer (ESO) to estimate the disturbances and uncertainties so that the uncertainties and exogenous disturbance are grouped into a single state called, the “total disturbance” or “generalized disturbance”, which is estimated and cancelled in real-time fashion via the ESO. ADRC is a combination of three essential elements: State Error Feedback (SEF) controller, an ESO, and a Tracking Differentiator(TD).

Moreover, the controller in the feedforward loop will work entirely for the stabilization of the nonlinear system (Chang et al., 2016; Dou, et al, 2017. Kong and Wen, 2017; Ma and Jiao, 2017). Model Predictive Control (MPC) enhanced by external forces are proposed and designed (Kocer, B. B. et al., 2019). (Razmi and Afshinfar, 2019) proposed a method for the position and attitude tracking control of a quadrotor UAV which combines a neural network adaptive scheme with sliding mode control. Backstepping control technique has been investigated to design optimal motion control for the quadrotor system (Saud and Hasan, 2018). The work of (Abbas and Sami, 2018) demonstrated the design and implementation of a PID controller for the motion control of a real quadrotor. Moreover, the work included a new swarm optimization algorithm for the parameters tuning of the PID controller using Cultural Exchange Imperialist Competitive Algorithm.

In some of the aforementioned studies, the control design was based on the approximate modeling of the nonlinear quadcopter UAV system (either a linearized modeling or an incomplete nonlinear model) while other studies didn't take into consideration the uncertainties in the system and how to deal with them. Motivated by the above researches, in this paper, a control system for the 6-

DoF quadrotor system is proposed and consists of four IADRCs, one for altitude subsystem and the other three for attitude subsystems. Each IADRC unit comprises of an Improved Tracking Differentiator (ITD) and a NonLinear PID (NLPID) controller, while the ESO was of linear type.

The main contributions of this paper are fourfold, first, an Improved ADRC (IADRC) scheme is constructed for UAV 6-DoF quadrotor system which is a highly coupled under-actuated MIMO system based on an Improved State Error Feedback (ISEF) and Improved Tracking Differentiator (ITD). Second, the complete nonlinear mathematical model of the 6-DoF quadrotor UAV system has been adopted in the design and stability analysis of the IADRC configuration. Third, a new multiobjective Output Performance Index (OPI) has been proposed and included in the parameters design of the IADRC structure; it minimizes the integrated time absolute error, controller energy, and integrated time absolute of the control signal. Finally, a detailed stability analysis for the closed-loop control system of the nonlinear 6-DoF quadrotor UAV system using Hurwitz stability theorem has been introduced to emphasize the validity of the proposed control scheme.

The rest of the paper is organized as follows: Section 2 discusses the quadrotor mathematical model, while the problem is stated in Section 3. The IADRC design is given in Section 4. Next, Section 5 presents the stability analysis for the Linear Extended State observer (LESO) and the closed-loop quadrotor system. The main results of simulations are presented and discussed in Section 6. Finally, Section 7 introduces the conclusions and future work.

2. QUADROTOR MATHEMATICAL MODEL

Quadrotors are a 6-DOF UAV with four rotors; this makes one uses a combination of rotors' speeds (Ω) to represent each DOF. **Fig. 1** shows all possible movements for the quadrotor. The quadrotor mathematical model, according to Newton-Euler equation is shown in (1) and (2). All parameters used are as follows, $[x \ y \ z]$ is the linear position vector (meter), d is the drag coefficient (N.m.sec²), l is the distance from the center to the motor (meter), b is the thrust coefficient (N.sec²), $[\Omega_1 \ \Omega_2 \ \Omega_3 \ \Omega_4]$ is the rotors speed vector (rad/sec), m is the total mass (Kg), g is the gravitational force (m/sec²), $[\tau_{wx} \ \tau_{wy} \ \tau_{wz}]$ is the Wind torque vector (N.m), $[f_{wx} \ f_{wy} \ f_{wz}]$ is the wind force vector (N), $[\tau_x \ \tau_y \ \tau_z]$, is the control torques (N.m), f_t is the total thrust of rotors (N), $[I_x \ I_y \ I_z]$ is the moment of inertia vector (Kg.m²), $[p \ q \ r]$ is the Angular velocity vector (rad/sec), $[\phi \ \theta \ \psi]$ is the Angular position vector (rad). For a more detailed derivation of the quadrotor mathematical model refer to (**Sabatino, 2015**). The force and torques that act on the 6-DOF quadrotor UAV system are described as follows,

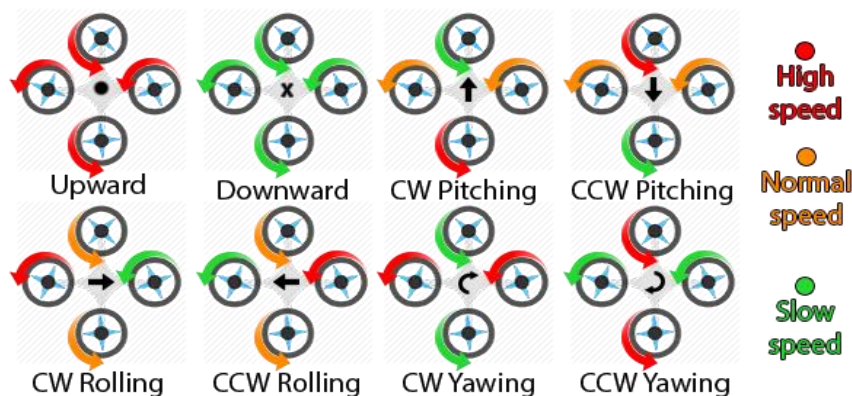


Figure 1. Quadrotor movements.



$$\begin{cases} f_t = b(\Omega_1^2 + \Omega_2^2 + \Omega_3^2 + \Omega_4^2) \\ \tau_x = bl(\Omega_3^2 - \Omega_1^2) \\ \tau_y = bl(\Omega_4^2 - \Omega_2^2) \\ \tau_z = d(\Omega_2^2 + \Omega_4^2 - \Omega_1^2 - \Omega_3^2) \end{cases} \quad (1)$$

while the nonlinear state-space model of the 6-DoF quadrotor UAV system is given as,

$$\begin{cases} \dot{x} = c(\psi)c(\theta)u + [c(\psi)s(\phi)s(\theta) - c(\phi)s(\psi)]v + [s(\phi)s(\psi) + c(\phi)c(\psi)s(\theta)]\omega \\ \dot{u} = rv - q\omega - gs(\theta) + \frac{f_{wx}}{m} \end{cases} \quad (2.a)$$

$$\begin{cases} \dot{y} = c(\theta)s(\psi)u + [c(\phi)s(\psi) + s(\phi)s(\psi)s(\theta)]v + [c(\phi)s(\psi)s(\theta) - c(\psi)s(\phi)]\omega \\ \dot{v} = -ru + p\omega + gs(\phi)c(\theta) + \frac{f_{wy}}{m} \end{cases} \quad (2.b)$$

$$\begin{cases} \dot{z} = -s(\theta)u + c(\theta)s(\phi)v + c(\phi)c(\theta)\omega \\ \dot{\omega} = qu - pv + gc(\theta)c(\phi) + \frac{f_{wz} - f_t}{m} \end{cases} \quad (2.c)$$

$$\begin{cases} \dot{\phi} = p + s(\phi)t(\theta)q + c(\phi)t(\theta)r \\ \dot{p} = \frac{I_y - I_z}{I_x}rq + \frac{\tau_x + \tau_{wx}}{I_x} \end{cases} \quad (2.d)$$

$$\begin{cases} \dot{\theta} = c(\phi)q - s(\phi)r \\ \dot{q} = \frac{I_z - I_x}{I_y}pr + \frac{\tau_y + \tau_{wy}}{I_y} \end{cases} \quad (2.e)$$

$$\begin{cases} \dot{\psi} = \frac{s(\phi)}{c(\theta)}q + \frac{c(\theta)}{c(\phi)}r \\ \dot{r} = \frac{I_x - I_y}{I_z}pq + \frac{\tau_z + \tau_{wz}}{I_z} \end{cases} \quad (2.f)$$

where $c(\cdot) \equiv \cos(\cdot)$, $s(\cdot) \equiv \sin(\cdot)$, and $t(\cdot) \equiv \tan(\cdot)$.

3. PROBLEM STATEMENT

The mathematical model given by (2) represents a quadcopter which is exposed to different uncertainties in its parameters such as its mass (m) or moments of inertia (I_x, I_y, I_z), and different exogenous disturbances, for example, the air or collision with another body. Our problem is to design the control law $v = [f_t \ \tau_x \ \tau_y \ \tau_z]$ which has to be generated in such a way that achieves stabilization for the quadrotor 6-DOF nonlinear UAV plant, abolish different exogenous disturbances $D(t) = [f_{wx} \ f_{wy} \ f_{wz} \ \tau_{wx} \ \tau_{wy} \ \tau_{wz}]$ and uncertainties that the quadcopter plant exhibits, and minimize the multi-objective OPI that reflects the optimal time-domain requirements and minimal control energy consumption for trajectory tracking and altitude and attitude positioning.

4. Improved Active Disturbance Rejection Control (IADRC) DESIGN

ADRC, in general, is a combination of a nonlinear controller (e.g., SEF), and the signal profile generator (e.g., TD), and state and total disturbance observer (e.g., LESO). Each one of these

components has its features as listed below. The structure of the general IADRC is shown in **Fig. 2**. In this paper, four second-order IADRC units for the 6-DoF quadrotor system will be designed, one for the altitude (z) subsystem, and three units for the attitude (ϕ, θ , and ψ) subsystems. The LESO of IADRC unit estimates the states up to the relative degree (ρ) of each subsystem and is equal to two for the quadrotor subsystems.

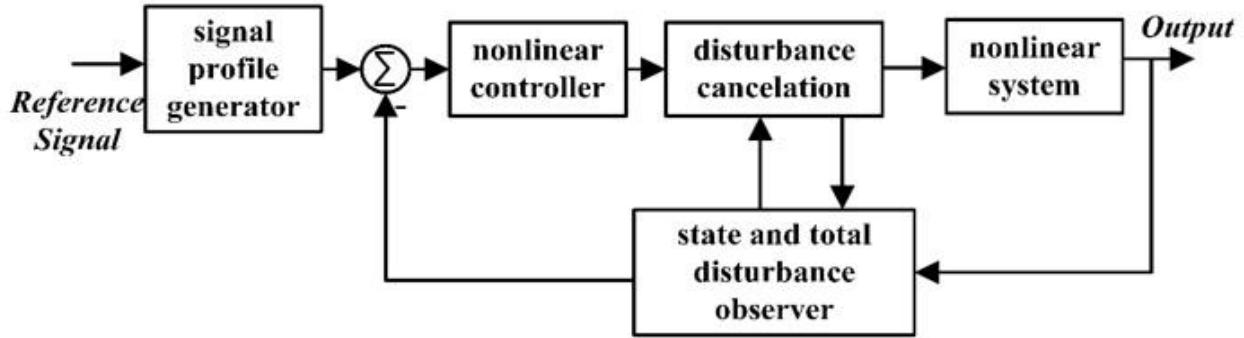


Figure 2. IADRC structure.

The main three units of the proposed IADRC of **Fig. 2** are:

1. An Improved Tracking Differentiator (ITD)

It is referred to as the signal profile generator in **Fig. 2** and designed to deal with transitioning and reproduce the reference signal and its derivative. The ITD is proposed as,

$$\begin{cases} \dot{r}_1 = r_2, r_1(0) = r_{10} \\ \dot{r}_2 = -a \left(\frac{\exp(\frac{m}{\gamma}) - \exp(-\frac{m}{\gamma})}{\exp(\frac{m}{\gamma}) + \exp(-\frac{m}{\gamma})} \right) + b r_2, r_1(0) = r_{20} \end{cases} \quad (3)$$

where $m = \beta r_1 - (1 - \alpha)r$, $a = R^2$, $b = -R$, r_1 is the output signal which tracks the reference signal r , r_2 tracks \dot{r} , the differentiated signal of r . The parameters R, β, α , and γ are design parameters, and they are optimized to give the best tracking results.

2. Linear Extended State Observer (LESO)

It is designed to estimate and observe the disturbances and uncertainties. Also, it is called the state and total disturbance observer in **Fig. 2**. The LESO equations used in the design are proposed as in (4),

$$\begin{cases} \dot{z}_1 = z_2 + \beta_1 e \\ \dot{z}_2 = z_3 + \beta_2 e + b_o U \\ \dot{z}_3 = \beta_3 e \end{cases} \quad (4)$$

where $e = (y - z_1)$, $\beta_1 = 3\omega_o$, $\beta_2 = 3\omega_o^2$, $\beta_3 = \omega_o^3$, ω_o is the bandwidth of the observer and should be optimized to give minimum estimation error, z_1, z_2 are the estimated states of the nonlinear system, while z_3 is the estimated total disturbance which represents the unwanted dynamics, uncertainties and exogenous disturbances.

3. Improved State Error Feedback (ISEF)

Also, it is denoted as the nonlinear controller as in **Fig. 2**. After estimating the total disturbance z_3 by the LESO, the ISEF minimizes the error and gives better performance for the system. A modified version of the NLPID controller is adopted by neglecting the integrator part, the new controller will be a NonLinear Proportional Derivative (NLPD) controller. The idea of ignoring the integrator part originates from the fact that the LESO will estimate all the uncertainties and exogenous disturbances and any other discrepancies in the system and eliminate them from the nonlinear system by subtracting these estimated unwanted signals from the input channel is a real-time behavior. The result is a linearized system with a chain of integrators up to nonlinear system's relative degree (ρ), and the integrator action is already included in the system. The suggested NLPD controller is constructed as

$$\begin{cases} u_{NLPD} = g_1(e) + g_2(\dot{e}) \\ g_i(\epsilon) = (k_{i1}\epsilon|\epsilon|^{\alpha_i-1}(1 + \exp(\mu_i\epsilon^2)) + k_{i2}\epsilon|\epsilon|^{\alpha_i-1}) p(\epsilon), i \in \{1,2\} \end{cases} \quad (5)$$

where $p(\epsilon) = 1/(1 + \exp(\mu_i\epsilon^2))$, ϵ could be one of e or \dot{e} . The net control signal that actuates the nonlinear system after subtracting the total disturbance from the input channel is given as,

$$U = u_{NLPD} - \frac{z_3}{b_o} \quad (6)$$

The quadrotor system is a multi-loop system as shown in **Fig. 3**. The position (x, y) controllers are simply NLPID controllers without ADRC compensation because there are no real control signals in their model equations. In this paper, our interest will be the altitude (z) and attitude (ϕ, θ , and ψ) systems.

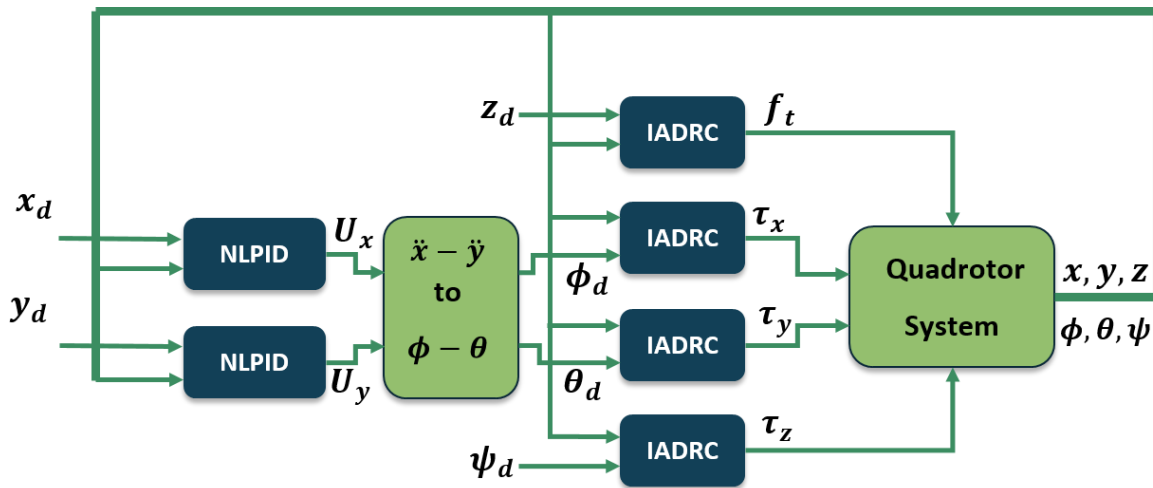


Figure 3. Quadrotor System with IADRC configuration.

5. QUADROTOR SYSTEM STABILITY ANALYSIS

The overall closed-loop stability analysis for the translational (altitude (z)) and rotational (attitude (ϕ, θ, ψ)) subsystems with the IADRCs is proved in this section by using Hurwitz stability theorem. As can be seen from the systems' equations stated in (2) they cannot be represented by a chain of integrators, so a transformation is derived below and used to accommodate the



nonlinearities of the 6-DoF quadrotor subsystems where the nonlinearities appear in a different channel of the control signal. On the other hand, the exogenous disturbance acts on the same channel of the control signals for these four quadrotor subsystems (matched disturbance case). Each of the four systems (\mathbf{z} , $\boldsymbol{\phi}$, $\boldsymbol{\theta}$, and $\boldsymbol{\psi}$) can be represented by

$$\begin{cases} \dot{\zeta}_1 = F_1(\zeta) \\ \dot{\zeta}_2 = F_2(\zeta) + b_1U + b_2d \\ \Gamma = \zeta_1 \end{cases} \quad (7)$$

where ζ is the states of the quadrotor system, b_1, b_2 are constants coefficients, F_1, F_2 are nonlinear functions, U is the control signal for this subsystem, d is the exogenous disturbance. Finally, Γ is the output of the system. By differentiating the first equation of (7) w.r.t t , one gets,

$$\ddot{\zeta}_1 = \frac{\partial F_1(\zeta)}{\partial \zeta_1} \dot{\zeta}_1 + \frac{\partial F_1(\zeta)}{\partial \zeta_2} \dot{\zeta}_2 \quad (8)$$

Substitute equations (7) in equation (8) one gets,

$$\ddot{\zeta}_1 = \frac{\partial F_1(\zeta)}{\partial \zeta_1} F_1(\zeta) + \frac{\partial F_1(\zeta)}{\partial \zeta_2} (F_2(\zeta) + b_1U + b_2d) \quad (9)$$

Simplifying (9), results in,

$$\ddot{\zeta}_1 = F_{total}(\zeta) + b_1 \frac{\partial F_1(\zeta)}{\partial \zeta_2} U + b_2 \frac{\partial F_1(\zeta)}{\partial \zeta_2} d \quad (10)$$

where $F_{total} = \frac{\partial F_1(\zeta)}{\partial \zeta_1} F_1(\zeta) + \frac{\partial F_1(\zeta)}{\partial \zeta_2} F_2(\zeta)$. Letting $\tilde{b}_1 = b_1 \frac{\partial F_1(\zeta)}{\partial \zeta_2}$, $\tilde{b}_2 = b_2 \frac{\partial F_1(\zeta)}{\partial \zeta_2}$, then,

$$\ddot{\zeta}_1 = F_{total} + \tilde{b}_1 U + \tilde{b}_2 d \quad (11)$$

Let $\tilde{\zeta}_1 = \zeta_1$ and $\tilde{\zeta}_2 = \dot{\zeta}_1$, then,

$$\begin{cases} \dot{\tilde{\zeta}}_1 = \tilde{\zeta}_2 \\ \dot{\tilde{\zeta}}_2 = F_{total} + \tilde{b}_1 U + \tilde{b}_2 d + b_o U - b_o U \\ \Gamma = \tilde{\zeta}_1 \end{cases} \quad (12)$$

where b_o is an approximation to \tilde{b}_1 within $\pm 50\%$ (Han, 2009). As can be seen from (12) that the nonlinearities have been moved into the same channel of the control signal. Furthermore, letting

$$\tilde{\zeta}_3 = L = F_{total} + \tilde{b}_2 d + (\tilde{b}_1 - b_o)U + \tilde{b}_2 d \quad (13)$$

be the “total disturbance” and substituting in (12), yields,

$$\begin{cases} \dot{\tilde{\zeta}}_1 = \tilde{\zeta}_2 \\ \dot{\tilde{\zeta}}_2 = \tilde{\zeta}_3 + b_o U \\ \dot{\tilde{\zeta}}_3 = \dot{L} \\ \Gamma = \tilde{\zeta}_1 \end{cases} \quad (14)$$



The above representation of (14) is called *Brunovsky form (BF)*.

Assumption (A1). The total disturbance fulfills the following,

1. $\sup_{0 \leq t \leq \infty} L(t) \leq M_1.$
2. $\sup_{0 \leq t \leq \infty} \dot{L}(t) \leq M_2.$
3. $\lim_{t \rightarrow \infty} L(t) = N$
4. $\lim_{t \rightarrow \infty} \dot{L}(t) = \lim_{t \rightarrow \infty} \frac{d\tilde{\zeta}_3}{dt} = 0$

where $M_1, M_2,$ and N are positive constants.

Theorem 1. Given any of the nonlinear 6-DoF quadrotor subsystems (2.a-2.f) represented in Brunovsky Form as a chain of integrators given in (14) and the LESO described by (4). If assumption A1 holds, then the LESO converges asymptotically to the 6-DoF quadrotor subsystems (2.a-2.f) expressed in (13). Moreover, the estimation errors $e_j = (\tilde{\zeta}_j - z_j), j \in \{1,2,3\}$ approach zero if the LESO coefficients $\beta_j, j \in \{1,2,3\}$ are chosen such that the polynomial $s^3 + \beta_1 s^2 + \beta_2 s + \beta_3$ is Hurwitz stable.

Proof: The error dynamics of the LESO e_i can be found by the following equations

$$\begin{cases} e_1 = \tilde{\zeta}_1 - z_1 \\ e_2 = \tilde{\zeta}_2 - z_2 \\ e_3 = \tilde{\zeta}_3 - z_3 \end{cases} \tag{15}$$

By substituting (4) and (14) in the derivative of (15), results in,

$$\begin{cases} \dot{e}_1 = \tilde{\zeta}_2 - z_2 - \beta_1 e_1 \\ \dot{e}_2 = \tilde{\zeta}_3 + b_o U - z_3 - \beta_2 e_1 - b_o U \\ \dot{e}_3 = \dot{L} - \beta_3 e_1 \end{cases} \tag{16}$$

and is expressed in another form as,

$$\begin{cases} \dot{e}_1 = e_2 - \beta_1 e_1 \\ \dot{e}_2 = e_3 - \beta_2 e_1 \\ \dot{e}_3 = \dot{L} - \beta_3 e_1 \end{cases} \tag{17}$$

In matrix form, the dynamics of (17) can be written as,

$$\dot{\mathbf{e}} = A_S \mathbf{e} + A_T \dot{L} \tag{18}$$

where

$$A_S = \begin{bmatrix} -\beta_1 & 1 & 0 \\ -\beta_2 & 0 & 0 \\ -\beta_3 & 0 & 0 \end{bmatrix}, A_T = \begin{bmatrix} 0 \\ 0 \\ 1 \end{bmatrix}, \mathbf{e} = \begin{bmatrix} e_1 \\ e_2 \\ e_3 \end{bmatrix}$$



If condition (4) in Assumption A1 satisfied, then, the second term will vanish. The matrix A_S with the characteristic equation $\lambda^3 + \beta_1\lambda^2 + \lambda\beta_2 + \beta_3$ is Hurwitz stable if the coefficients $\beta_j, j \in \{1,2,3\}$ satisfy the conditions of the Routh-Hurwitz Criterion conditions, *i.e.*, $\beta_1, \beta_2, \beta_3 > 0$ and $\beta_1\beta_2 > \beta_3$. Hence, the system of (18) is asymptotically stable and the errors $e_j, j \in \{1,2,3\}$ decay zero and the LESO approaches asymptotically to (14).

Assumption (A2). The ITD of (3) tracks a reference signal r with a very small error and with

$$\ddot{r}^{(2)} = 0, \text{ i.e., } \lim_{t \rightarrow \infty} (\ddot{r}^{(i-1)} - \ddot{r}_i) = 0, i \in \{1,2\}.$$

Assumption (A3). The LESO of (4) perfectly estimates the states of the nonlinear system, *i.e.*,

$$\lim_{t \rightarrow \infty} e_i = 0, i = 1,2,3$$

Assumption (A4). The values of α_i of the NLPD controller (5) are approximately set to unity, *i.e.*,

$$\alpha_1 \approx \alpha_2 \approx 1$$

which makes the mathematical relation of $g_i(\epsilon)$ in (5) expressed as,

$$g_i(\epsilon) = (k_{i1}(1 + \exp(\mu_i\epsilon^2)) + k_{i2}) \epsilon p(\epsilon) = \dot{g}_i(\epsilon) \epsilon$$

where ϵ could be one of e or \dot{e} , $\dot{g}_i(\epsilon) = (k_{i1}(1 + \exp(\mu_i\epsilon^2)) + k_{i2})p(\epsilon)$, $i \in \{1,2\}$, which is a sector bounded positive function, *i.e.*, $g_i(\epsilon) \in [k_{i1}, k_{i1} + k_{i2}/2]$.

Theorem 2. Given any of the nonlinear 6-DoF quadrotor subsystems (2.a-2.f) represented in Brunovsky form as in (14) and the IADRC which consists of the ITD, LESO, and ISEF (*i.e.*, NLPD) described in (3), (4), and (5) respectively. Knowing that Assumptions A1, A2, A3, and A4 hold, then, the closed-loop system is asymptotically Hurwitz stable provided that the nonlinear gains $\dot{g}_i(\tilde{e}_i), i \in \{1,2\}$ are chosen such that the characteristic equation $s^2 + \dot{g}_2(\epsilon)s + \dot{g}_1(\epsilon)$ is Hurwitz stable.

Proof: The closed-loop error dynamics of the system (14) are written as

$$\begin{cases} \dot{\tilde{e}}_1 = \ddot{r} - z_1 \\ \dot{\tilde{e}}_2 = \dot{\ddot{r}} - z_2 \end{cases}$$

After convergence of the LESO and assume that the assumption A3 holds, then, the closed-loop error dynamics of the system can be found as

$$\begin{cases} \dot{\tilde{e}}_1 = \ddot{r} - \tilde{\zeta}_1 \\ \dot{\tilde{e}}_2 = \dot{\ddot{r}} - \tilde{\zeta}_2 \end{cases} \tag{19}$$

Differentiating both side yields,



$$\begin{cases} \dot{\tilde{e}}_1 = \dot{r} - \dot{\tilde{\zeta}}_1 \\ \dot{\tilde{e}}_2 = \dot{r} - \dot{\tilde{\zeta}}_2 \end{cases} \quad (20)$$

For the system of (14), the states $\tilde{\zeta}_i, i \in \{1,2\}$ can be expressed in terms of the nonlinear output, $\tilde{\zeta}_i = y^{(i-1)}, i \in \{1,2\}$. If assumptions A2 holds, then, the error dynamics of (20) will be given as

$$\begin{cases} \dot{\tilde{e}}_1 = \tilde{e}_2 \\ \dot{\tilde{e}}_2 = -z_2 - b_0 U \end{cases} \quad (21)$$

With $U = u_{NLPD} - \frac{z_3}{b_0}$

$$\begin{cases} \dot{\tilde{e}}_1 = \tilde{e}_2 \\ \dot{\tilde{e}}_2 = -z_3 - u_{NLPD} + z_3 \end{cases} \quad (22)$$

Canceling z_3 results in

$$\begin{cases} \dot{\tilde{e}}_1 = \tilde{e}_2 \\ \dot{\tilde{e}}_2 = -u_{NLPD} \end{cases} \quad (23)$$

By substituting u_{NLPD} in (5), yields,

$$\begin{cases} \dot{\tilde{e}}_1 = \tilde{e}_2 \\ \dot{\tilde{e}}_2 = -[g_1(e_1) + g_2(e_2)] \end{cases} \quad (24)$$

If assumption A4 is valid, then,

$$\begin{cases} \dot{\tilde{e}}_1 = \tilde{e}_2 \\ \dot{\tilde{e}}_2 = -\dot{g}_1(e_1)e_1 - \dot{g}_2(e_2)e_2 \end{cases} \quad (25)$$

In matrix form,

$$\dot{\tilde{e}} = A_C \tilde{e} \quad (26)$$

where A_C is given as

$$A_C = \begin{bmatrix} 0 & 1 \\ -\dot{g}_1(e_1) & -\dot{g}_2(e_2) \end{bmatrix}$$

With the characteristic equation $s^2 + \dot{g}_2(e_2)s + \dot{g}_1(e_1)$. The Hurwitz matrix H_o for A_C is given as

$$H_o = \begin{bmatrix} \dot{g}_2(e_2) & 0 \\ 1 & \dot{g}_1(e_1) \end{bmatrix} \quad (27)$$

From (27), it can easily derive the conditions for Hurwitz stability,



$$|\dot{g}_2(e_2)| = \dot{g}_2(e_2) > 0 \ \& \ \dot{g}_2(e_2)\dot{g}_1(e_1) > 0$$

The above conditions are already satisfied since $\dot{g}_2(e_2)$ and $g_1(e_1)$ are sector bounded positive functions, $g_i(\epsilon) \in [k_{i1}, k_{i1} + k_{i2}/2]$, $i \in \{1,2\}$ which proves the theorem.

6. SIMULATION AND RESULTS

The quadrotor model with the IADRC is implemented using MATLAB/Simulink environment with sampling time $T = 0.01$ sec, and all the results are discussed in parallel with that of the LPID and NLPID controllers. The 6-DoF quadrotor system parameters used in the simulation environment are given in the appendix. The optimum values of the IADRC unit’s parameters are obtained via the minimization problem of the multi-objective OPI index using Genetic Algorithm (GA) optimization as illustrated below,

$$OPI = \sum_j \hat{\gamma}_j \times [\gamma_{1j} \times UABS + \gamma_{2j} \times USQR + \gamma_{3j} \times ITAE] \tag{28}$$

for $j = z, \theta, \phi, \psi$ where *ITAE* is the Integrated Time Absolute error given as, $\int_0^{t_f} t|\tilde{e}|dt$, *USQR* is the Control Signal Energy, $\int_0^{t_f} |u_{NLPD}(t)|^2 dt$, and *UABS* is the Integrated absolute control signal expressed as, $\int_0^{t_f} |u_{NLPD}(t)| dt$, where t_f is the time interval of the simulation, γ_{1j} , γ_{2j} , and γ_{3j} are weighting parameters defined as the relative importance of one objective as compared to the other. They must satisfy $\gamma_{1j} + \gamma_{2j} + \gamma_{3j} = 1$. The same applies for $\hat{\gamma}_j$ with a relative importance of one subsystem as compared to other subsystems. All the IADRCs parameters are shown in Tables (1-4). It is worth to mention that the tuning processing is achieved in an off-line manner, i.e., all the parameters of all three IADRC units are tuned using GA according to (28) firstly, then, they are kept constant during the simulation period. Any discrepancies, uncertainties, and exogenous disturbances that the 6-DoF UAV system may exhibit will, in turn, be accounted for by the LESO, which will estimate all these unwanted factors and cancel them from the input channel in an online manner. Moreover, the sampling time used to calculate

Table 1. ESOs parameters

parameter	z subsystem	ϕ subsystem	θ subsystem	ψ subsystem
ω_o	300	861.36	671.76	749.05
b_o	0.5	0.004	0.005	0.004

Table 2. ITDs parameters

parameters	z, ϕ, θ, ψ subsystems
α	0.978
β	2.793
γ	16.772
R	26.50



Table 3. ISEF parameters

parameter	z subsystem	ϕ subsystem	θ subsystem	ψ subsystem
k_{11}	32.480	5.639	5.108	0.699
k_{12}	11.436	0.076	0.039	0.210
k_{21}	9.075	0.749	0.066	0.241
k_{22}	0.141	0.047	0.066	0.102
μ_1	0.281	0.076	0.519	0.127
μ_2	0.423	0.599	0.774	0.376
α_1	0.968	0.959	0.957	0.974
α_2	0.958	0.954	1.003	0.941

Table 4. PID controllers' parameters

parameter	z subsystem	ϕ subsystem	θ subsystem	ψ subsystem
k_P	67.599	1.090	1.280	1.406
k_D	11.718	0.068	0.110	0.230
k_I	76.339	0.560	0.803	1.424

6.1 Study Case One (Tracking)

The first test is to check the effectiveness of the IADRC for the 6-DoF quadrotor system to track time-varying reference signals. For each of the four subsystems, the following reference input has been applied while a constant step reference input is imposed for the rest three subsystems,

$$r = u(t - 1) + 5u(t - 10) + 10u(t - 25) - 7u(t - 35) - 8u(t - 40) \tag{29}$$

Figs. 4-7 show the time response for the altitude subsystem z , and the attitude subsystems (ϕ, θ, ψ). The closed-loop errors occurred for all the states are always very small and reach zero after very a short time even the steps given at different times and different values.

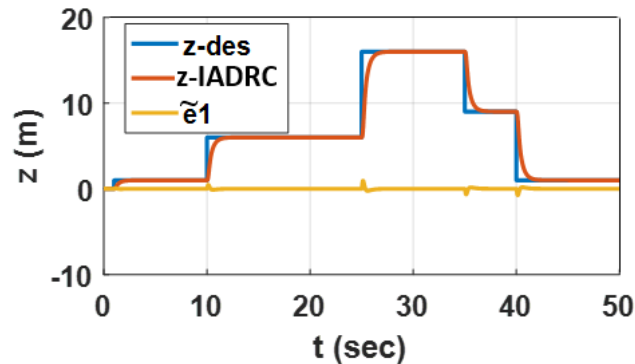


Figure 4. Altitude time response with the time-varying reference input.

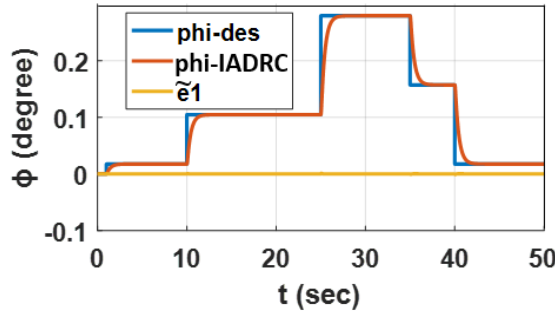


Figure 5. Roll time response with the time-varying reference input.

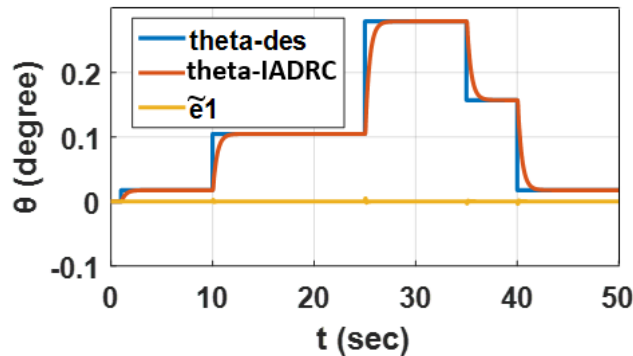


Figure 6. Pitch time response with the time-varying reference input.

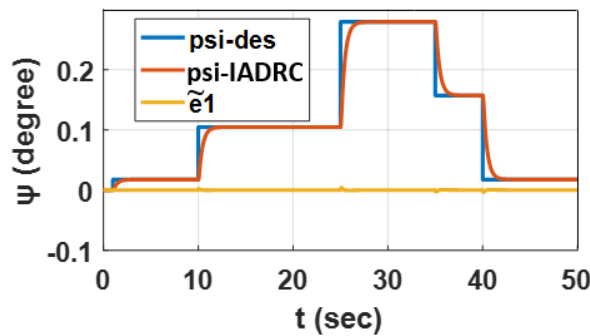


Figure 7. Yaw time response with the time-varying reference input.

6.2 Study Case two (Disturbance Rejection)

Disturbance rejection was the last test demonstrated with the IADRC configuration on the 6-DoF quadrotor system was to ensure stable and accurate tracking in the presence of exogenous disturbances. This test has been achieved by applying several disturbances at different times on the attitude(ϕ, θ, ψ)subsystems. The disturbances values applied are $[0.5, 0.5, 0.5] N.m$ at $[10, 25, 35] sec$ respectively and the time responses of the attitude states are shown in **Figs. 8-10**. The output response is deteriorated using LPID and NLPID controllers with large overshoots of more than 200% of the steady-state response, while the IADRC rejected the disturbances very quick and with very small peak values.

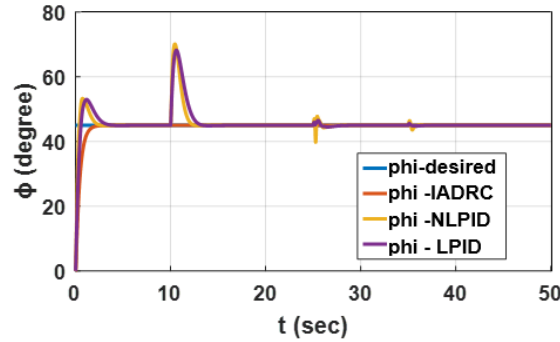


Figure 8. Roll time response with disturbances.

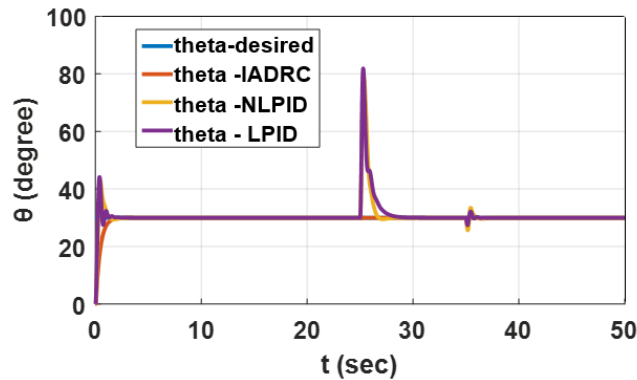


Figure 9. Pitch time response with disturbances.

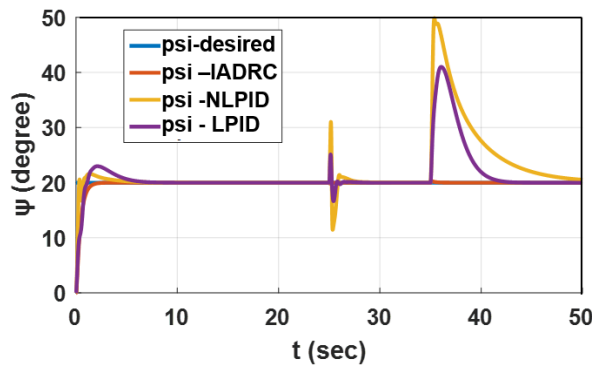


Figure 10. Yaw time response with disturbances.

6.3 Study Case three (Uncertainties Rejection)

The third test was chosen to observe the effect of the uncertainties of the parameters on the output response of the 6-DoF quadrotor systems using the IADRC scheme. One of the settings that could face a significant change in its value is the mass m of the quadrotor. **Fig. 11** shows the response of the altitude (z) with an uncertainty of $\Delta_m = +100\%$ in the quadrotor mass occurred at $t = 25$ sec of the simulation time. As can be seen from **Fig. 11**, the ADRC tackled this uncertainty in the mass with a very small error, with less than 2% of the steady-state response. The other controllers used in the comparison exhibited high peaks and took a long time to get rid of the uncertainty effect.

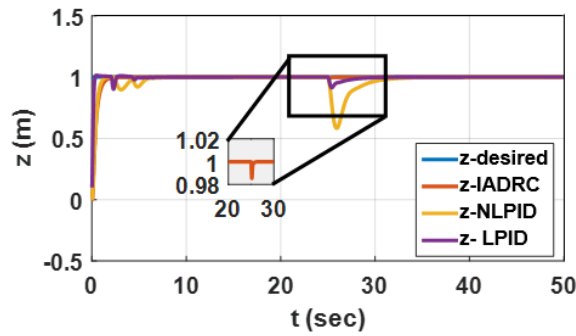


Figure 11. Altitude with uncertainty in the mass.

6.4 Study Case four (Decoupling)

The second test was to prove that the attitude subsystems are totally decoupled using the IADRC configuration. It is accomplished by applying a step reference input of 45° at $t = 5$ sec, while the other two subsystems have a constant step reference input of 10° . It is very clear from **Fig. 12** that the ADRCs perfectly decoupled the states while the NLPID and the LPID could not do that and a peak overshoot happens in one or more of the attitude states whenever there is a sudden change in the reference signals of the other subsystems. On the other hand, the IADRC gave a smooth and fast response without any interactions between different subsystems of the 6-DoF quadrotor systems.

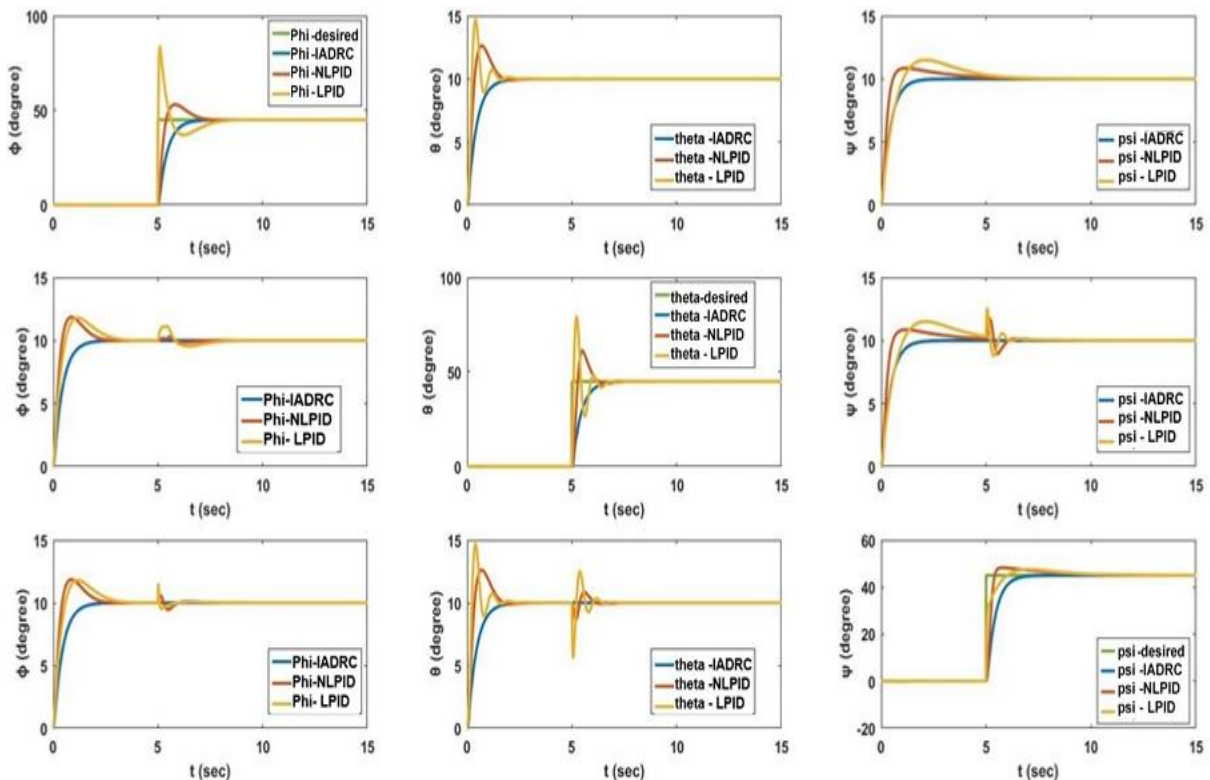


Figure 12. Attitude states decoupling.



6.5 Discussion

The effectiveness of the IADRC to achieve accurate tracking, decoupling and cancellation of the parameter uncertainties is due to the capability of the IADRC to consider these couplings between different quadrotor subsystems and system parameter variations as part of the total disturbance which is estimated and fed into the input channel for cancellation by the LESO. Moreover, the LESO ability to correctly predict the exogenous disturbance and canceling them from the nonlinear system’s input channel very quickly in a real-time manner is the principal justification for excellent reference tracking in the existence of the external disturbances. Finally, the LPID and NLPID controllers failed to achieve this task.

7. CONCLUSIONS

This work presented an IADRC for the stabilization and trajectory tracking control design for an under-actuated 6-DoF quadrotor UAV system. From the results, one can conclude that the IADRC has shown an excellent reference tracking and exogenous disturbance and uncertainties rejection with minimum ITAE, USQR, and UABS time-domain indices. Furthermore, the IADRC removed quadrotor subsystems interactions and converted these subsystems into simple double integrator subsystems, which positively improved the reference tracking and removed the steady-state errors. The Comparison with LPID and NLPID controllers demonstrated the validation and powerfulness of the proposed control scheme when applied on highly nonlinear and strongly coupled MIMO system such as 6-DoF quadrotor UAV system.

Appendix A

Table A. 6-DoF UAV parameters.

Parameter	description	value
<i>I_x</i>	Moment of inertia of the <i>x</i> - subsystem	$8.553 * 10^{-3} \text{kg.m}^2$
<i>I_y</i>	Moment of inertia of the <i>y</i> - subsystem	$8.553 * 10^{-3} \text{kg.m}^2$
<i>I_z</i>	Moment of inertia of the <i>z</i> -subsystem	$1.476 * 10^{-2} \text{kg.m}^2$
<i>g</i>	Gravitational acceleration	9.81m/sec^2
<i>m</i>	Mass	0.964kg
<i>b</i>	Thrust coefficient	$7.66 * 10^{-5} \text{N. sec}^2$
<i>d</i>	Drag coefficient	$5.63 * 10^{-6} \text{N. m. sec}^2$
<i>l</i>	Distance from center to motor	0.22 meter

REFERENCES

- Abbas, N. and Sami, A. (2018) “Tuning of PID Controllers for Quadcopter System using Cultural Exchange Imperialist Competitive Algorithm”, Journal of Engineering, 24(2), pp. 80-99. Available at: <http://joe.uobaghdad.edu.iq/index.php/main/article/view/526>.
- Abdullaha, A., Bakar, E. A., Pauzi M. Z. M., 2015. Monitoring of Traffic Using Unmanned Aerial Vehicle in Malaysia Landscape Perspective, Jurnal Teknologi, 76(1), pp. 367–372. DOI: 10.11113/jt.v76.4043.



- Aboudonia, A., Rashad, R. and El-Badawy, A., 2015. Time domain disturbance observer based control of a quadrotor unmanned aerial vehicle, in 2015 XXV International Conference on Information, Communication and Automation Technologies (ICAT). Sarajevo, Bosnia Herzegovina: IEEE, pp. 1–6. DOI: 10.1109/ICAT.2015.7340501.
- Belyavskiy, A.O., Tomashevich, S. I., Andrievsky, B., 2017. Application of 2DOF Quadrotor-based Laboratory Testbed for engineering education, in 25th Mediterranean Conference on Control and Automation (MED). Valletta, Malta: IEEE, pp. 939–944. DOI: 10.1109/MED.2017.7984240.
- Chang, K., Xia, Y., Huang, K., Ma, D., 2016. Obstacle avoidance and active disturbance rejection control for a quadrotor, *Neurocomputing*. Elsevier, 190, pp. 60–69. DOI: 10.1016/J.NEUCOM.2016.01.033.
- Dhivya, A. J. A., Premkumar, J., 2017. Quadcopter based technology for an emergency healthcare, in Third International Conference on Biosignals, Images and Instrumentation (ICBSII), Chennai, India, IEEE, pp. 1–3. DOI: 10.1109/ICBSII.2017.8082284.
- Dou, J., Kong, X. and Wen, B., 2017. Altitude and attitude active disturbance rejection controller design of a quadrotor unmanned aerial vehicle, *Proceedings of the Institution of Mechanical Engineers, Part G: Journal of Aerospace Engineering*, 231(9), pp. 1732–1745. DOI: 10.1177/0954410016660871.
- Han, J. H. J., 2009. From PID to Active Disturbance Rejection Control, *IEEE Transactions on Industrial Electronics*, 56(3), pp. 900–906. DOI: 10.1109/TIE.2008.2011621.
- Jingjit, P., Mitsantisuk, C., Rungrangpitayagon, J., Teerakawanich, N., 2014. Quadrotor robot based on disturbance observer control, in TENCON 2014 - 2014 IEEE Region 10 Conference. Bangkok, Thailand: IEEE, pp. 1–6. DOI: 10.1109/TENCON.2014.7022400.
- Kocer, B. B., Tjahjowidodo, T., Seet, G. L., 2019. Model predictive UAV-tool interaction control enhanced by external forces, *Mechatronics*, (58), pp.47-57, DOI: 10.1016/j.mechatronics.2019.01.004.
- Ma, Z., Jiao, S. M., 2017. Research on the attitude control of quad-rotor UAV based on active disturbance rejection control, in 3rd IEEE International Conference on Control Science and Systems Engineering (ICCSSE). Beijing, China: IEEE, pp. 45–49. DOI: 10.1109/CCSSE.2017.8087892.
- Nathan, P. T., Almurib, H. A. F., Kumar, T. N., 2011, A review of autonomous multi-agent quadrotor control techniques and applications, in 4th International Conference on Mechatronics (ICOM). Kuala Lumpur, Malaysia: IEEE, pp. 1–7. DOI: 10.1109/ICOM.2011.5937132.



- Razmi, H., Afshinfar, S., 2019. Neural network-based adaptive sliding mode control design for position and attitude control of a quadrotor UAV, *Aerospace Science and Technology*, in press, DOI:10.1016/j.ast.2019.04.055.
- Sabatino, F., 2015. Quadrotor control: modeling, nonlinear control design, and simulation. Master's Degree Project, Royal Institute of Technology.
- Sahul, M. P. V., Chander, V. N. and Kurian, T., 2014. A novel method on Disturbance Rejection PID Controller for Quadcopter based on Optimization algorithm, *IFAC Proceedings Volumes*. Elsevier, 47(1), pp. 192–199. DOI: 10.3182/20140313-3-IN-3024.00016.
- Saud, L. and Hasan, A. (2018) “Design of an Optimal Integral Backstepping Controller for a Quadcopter”, *Journal of Engineering*, 24(5), pp. 46-65. DOI: 10.31026/j.eng.2018.05.04.
- Wang, H. and Chen, M., 2016. Trajectory tracking control for an indoor quadrotor UAV based on the disturbance observer, *Transactions of the Institute of Measurement and Control*, 38(6), pp. 675–692. DOI: 10.1177/0142331215597057.